

Annotation-free Audio-Visual Segmentation

Jinxiang Liu¹, Yu Wang^{1,2}, Chen Ju¹, Chaofan Ma¹, Ya Zhang^{1,2}✉, Weidi Xie^{1,2}✉

¹ Cooperative Medianet Innovation Center, Shanghai Jiao Tong University ² Shanghai AI Laboratory
{jinxliu, yuwangsJTU, ju.chen, chaofanma, ya-zhang, weidi}@sjtu.edu.cn

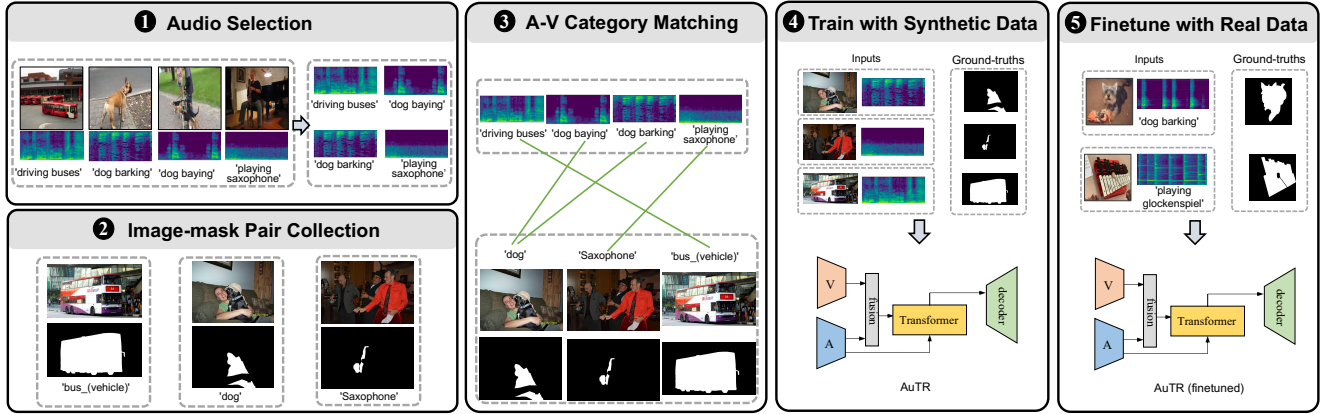


Figure 1: **Paper Overview.** First, we propose a pipeline for synthesizing datasets for audio-visual segmentation (AVS), by leveraging the *off-the-shelf* large image segmentation datasets, *e.g.*, COCO, LVIS, OpenImage, and audio datasets, *e.g.*, VGGSound. The pipeline is *annotation-free* and can easily be *scaled up* to cover more categories. Second, we propose a multi-modal transformer-based architecture for AVS task, termed as **AuTR** (Audio-aware TRansformer).

Abstract

is <https://jinxiang-liu.github.io/anno-free-AVS/>.

The objective of Audio-Visual Segmentation (AVS) is to locate sounding objects within visual scenes by accurately predicting pixelwise segmentation masks. In this paper, we present the following contributions: (i), we propose a scalable and annotation-free pipeline for generating artificial data for the AVS task. We leverage existing image segmentation and audio datasets to draw links between category labels, image-mask pairs, and audio samples, which allows us to easily compose (image, audio, mask) triplets for training AVS models; (ii), we introduce a novel Audio-Aware Transformer (AuTR) architecture that features an audio-aware query-based transformer decoder. This architecture enables the model to search for sounding objects with the guidance of audio signals, resulting in more accurate segmentation; (iii), we present extensive experiments conducted on both synthetic and real datasets, which demonstrate the effectiveness of training AVS models with synthetic data generated by our proposed pipeline. Additionally, our proposed AuTR architecture exhibits superior performance and strong generalization ability on public benchmarks. The project page

1. Introduction

Audio-visual segmentation (AVS) is a task that involves localizing and segmenting sounding objects in video frames using acoustic cues. Previous research has explored this task within the scope of self-supervised representation learning, often by leveraging co-occurring audio-visual signals [26, 25, 24, 35, 7, 50, 37, 49]. However, these training objectives lack fine-grained pixel-wise supervision, resulting in coarse segmentations, posing limitation to the applicability of AVS in real-world scenarios where accurate segmentations are required, such as video surveillance, multi-modal video editing, and the robotics industry.

To mitigate this challenge, Zhou *et al.* [68] tackled the issue of audio-visual segmentation through supervised learning, where they manually annotated a video dataset with pixel-level segmentations of sounding objects in video frames. However, this approach is not scalable due to the laborious annotation procedure. We propose an *annotation-free* and *scalable* pipeline for constructing artificial datasets for the AVS task. Our pipeline aims to resolve the issue

of insufficient training data and provides a more practical solution to the problem.

A crucial observation we have made is that a well-performing AVS model requires **dual-level** recognition ability. For instance, when presented with the sound of a dog barking, the model should first distinguish between semantic categories, such as dog versus cat, and then further resolve any instance ambiguity by identifying the specific dog marking the sound, only if multiple ones are present, such as dog-1 versus dog-2. In practice, the ability to distinguish semantic categories may have been sufficient for localising sounding objects in most daily scenarios, that can be achieved by training on artificially constructed data, without the need for additional manual annotations.

To train Audio-Visual Segmentation (AVS) models without relying on human annotation, we construct a synthetic dataset by leveraging off-the-shelf image segmentation and audio datasets, as illustrated in Figure 1. For instance, we can combine an image-mask pair labeled as “dog” from the image segmentation dataset LVIS with an audio sample labeled as “dog barking” from the audio dataset VGGSound to obtain an (*image*, *mask*, *audio*) triplet, which serves as a training sample for the AVS task. In this triplet, *image* and *audio* are the model inputs, and *mask* is the supervision for model outputs. Compared to the existing human-annotated dataset AVSBench [68], this dataset synthesis pipeline inherits annotations from computer vision communities, such as LVIS [19], Open Images [30], and SAM [29]. This pipeline requires zero extra annotation and can easily scale up to cover a large number of categories. Moreover, we propose a novel architecture for audio-visual segmentation called Audio-aware TRansformer (**AuTR**). It is a multi-modal transformer that features audio-aware learnable queries, that enable to perform effective cross-modal interaction and locate sounding objects with the guidance of audio information.

To summarize, our work makes the following contributions: (i), we introduce a novel and *scalable* pipeline to synthesize datasets for audio-visual segmentation at the semantic level, by exploiting the existing *off-the-shelf* large image segmentation and audio datasets. Experimentally, we demonstrate that models pre-trained on synthetic data can achieve satisfactory performance on existing AVS benchmarks, thus enabling zero-shot evaluation. Furthermore, after fine-tuning with a small number of paired image-mask data, performance can be further improved, demonstrating the effectiveness of our approach for data-efficient adaptation to real-world scenes. (ii), we propose an end-to-end multi-modal transformer framework to tackle the AVS problem. Our framework explicitly leverages audio information as learnable queries for the transformer decoder, iteratively attending to visual representations to obtain accurate segmentation for target sounding objects; (iii), ex-

tensive experiments demonstrate the effectiveness of our proposed Audio-aware TRansformer (AuTR) architecture for both single and multi-object AVS settings compared to existing methods. Additional evaluations also show that the proposed AuTR has stronger generalization abilities for open-set segmentation.

2. Related Work

Audio-visual segmentation. In the recent literature, researchers have explored a range of audio-visual tasks with the goal of getting a comprehensive understanding of multimedia resources. These tasks include audio-visual sound separation [65, 64, 17, 15, 54], visual sound source localisation [26, 25, 24, 35, 7, 50, 37, 49, 46] and audio-visual video understanding [28, 52, 36, 31, 52]. Visual sound source localisation (VSSL), or audio-visual segmentation, aim to localise and segment the sounding object regions based on its audio signals. Existing approaches [44, 67, 49, 7, 37] to this problem are primarily based on the co-occurrence of audio and visual signals, which provides only weak instance-level supervision, making it difficult to predict fine-grained pixel-level segmentation masks. To overcome this issue, Zhou *et al.* [68] have presented a dataset with two subsets where sounding objects in frames are annotated with binary masks, which is the first benchmark for supervised AVS tasks.

Transformer. Vanilla Transformer [55] was initially created to replace RNNs for the sequence-to-sequence machine translation problem in the NLP community, and quickly became the pillar framework for numerous NLP tasks due to its core attention mechanism, which grants it powerful long-range dependency modeling capabilities. In the recent literature, Transformer has also been adapted to tackle computer vision issues like image classification [6, 21, 5, 57, 56], image segmentation [38, 47], and video understanding [45, 2, 1]. Specifically, Nicolas *et al.* [4] introduced DETR, a query-based paradigm that employs the Transformer to achieve end-to-end object detection. This paradigm has been adopted to handle various problems such as detection [69, 20, 16, 13, 27], image segmentation [11, 66, 33, 12], video object tracking [10, 42, 51, 62], and video segmentation [3, 32, 61, 9, 60, 59]. Inspired by DETR, our method employs the query-based paradigm. Our proposed multi-modal Transformer is equipped with audio-aware learnable queries to generate segmentation masks based on the provided audio guidance. To the best of our knowledge, this is the first exploration to leverage one query-based transformer framework for the AVS task.

3. Method

In Section 3.1, we start by introducing the problem formulation; then we describe the procedure for constructing synthetic dataset in Section. 3.2; lastly, we detail the pro-

posed architecture in Section. 3.3.

3.1. Problem Formulation

For the task of audio-visual segmentation (AVS), the input data consists of a sequence of video frames, $\mathcal{V} = \{v_i\}_{i=1}^T$, where $v_i \in \mathbb{R}^{3 \times H_0 \times W_0}$, and its corresponding audios $\mathcal{A} = \{a_i\}_{i=1}^T$, where $a_i \in \mathbb{R}^{H_a \times W_a}$ refers to the corresponding audio spectrograms. The objective of AVS is to segment the sounding objects in each frame based on the acoustic cues. The target segmentation can be binary masks, *i.e.*, $\mathcal{M} = \{M_i\}_{i=1}^T$, and $M_i \in \{0, 1\}^{H_0 \times W_0}$.

3.2. AVS-Synthetic Dataset

As aforementioned, existing benchmark on audio-visual segmentation, *e.g.*, AVSBench [68], is collected by manually annotating frames with pixelwise segmentation masks, this is often expensive and only covers a limited number of categories (only 23). To remedy this, we introduce a scalable pipeline for constructing a synthetic dataset, termed as **AVS-Synthetic**. The dataset construction procedure leverages existing instance segmentation image datasets such as LVIS [19], Open Images [30], and audio classification dataset, such as VGGSound [8]. Thus this pipeline is free of extra manual annotations and can easily be scaled up.

3.2.1 Data Construction

Figure 1 shows our proposed pipeline for building a synthetic dataset for semantic-level audio-visual segmentation. Generally speaking, it consists of three steps:

(1) Audio Selection. We select audios using the instance-level class labels from publicly-released audio dataset, in this paper, we employ VGGSound [8], which is a large-scale audio-visual dataset collected using computer vision techniques, as a data source for sampling audio clips in our proposed AVS-Synthetic dataset. However, other audio datasets such as Audio Set [18] can also be used.

(2) Image-mask Pair Collection. Next, based on the category of selected audio clip, we pick the categorized image and segmentation mask pairs for the objects with the same category. This can easily be achieved by filtering the existing popular image segmentation datasets such as LVIS [19] and Open Images [30].

(3) Audio-Visual Category Matching. Till here, we have separately collected the audio and visual samples. We match the image-mask pairs with their corresponding audios to form the *(image, mask, audio)* triplet as a training sample for AVS task, where *(image, audio)* serve as model inputs and the *mask* is the ground-truth segmentation mask to supervise the model training. Matching these pairs is done by using the class labels of both image-mask pairs and the audio labels. Notably, different datasets may

have different class labels while referring to the same thing; such as *computer keyboard*: “computer_keyboard” (LVIS) and “typing on computer keyboard” (VGGSound); *dog*: “dog” (LVIS), “dog barking” (VGGSound) and “dog bay-ing” (VGGSound). Minimal manual verification is involved in this matching procedure.

3.2.2 Dataset Statistics

As an instantiation of our proposed *annotation-free* dataset collection pipeline for AVS, **AVS-Synthetic** dataset is proposed to cover 60,009 sounding object instances from 44 common categories. A detailed comparison between AVS-Synthetic and the human annotated AVSBench datasets [68] is listed in Table 1.

Dataset	Classes	Images	Masks	Data.Source	Human
AVSBench [68]	23	4932	10,852	[8]	✓
AVS-Synthetic (ours)	44	49,735	60,009	[19, 30, 8]	✗

Table 1: Comparison between our proposed AVS-Synthetic and AVSBench (S4) [68] datasets. AVSBench is collected with human annotations.

3.3. AuTR Framework

In addition to the automatic dataset construction, we propose a novel Audio-aware TRansformer (**AuTR**) architecture, as depicted in Figure 2, it consists of: visual encoder to extract compact visual features, audio encoder to extract audio features, audio-visual feature fusion module, multi-modal transformer with learnable audio-aware queries, a pixel decoder to generate multi-modal dense features and dynamic convolution block for final mask prediction.

3.3.1 Feature Extraction

Here, we detail the feature extraction procedure for both modality inputs, *i.e.*, video frames and audio spectrograms.

Visual Encoder. To extract dense visual features, we adopt pre-trained vision networks as backbone. In this paper, we experiment with either ImageNet pre-trained ResNet50 [22] or Pyramid Vision Transformer (PVT) [57]. To exploit features with rich semantic levels, we extract visual features of three different scales, denoted as $\mathcal{F}_v = \{[f_{v1}^t, f_{v2}^t, f_{v3}^t]\}_{t=1}^T$.

Audio Encoder. Given the corresponding audio clips $\mathcal{A} = \{a_i\}_{i=1}^T$, we compute its feature with a VGGish [23] model pretrained on AudioSet [18] dataset, then spatially pool the features into a vector, denoted as $\mathcal{F}_a = \{f_a^t\}_{t=1}^T$, where $f_a^t \in \mathbb{R}^{C_a}$.

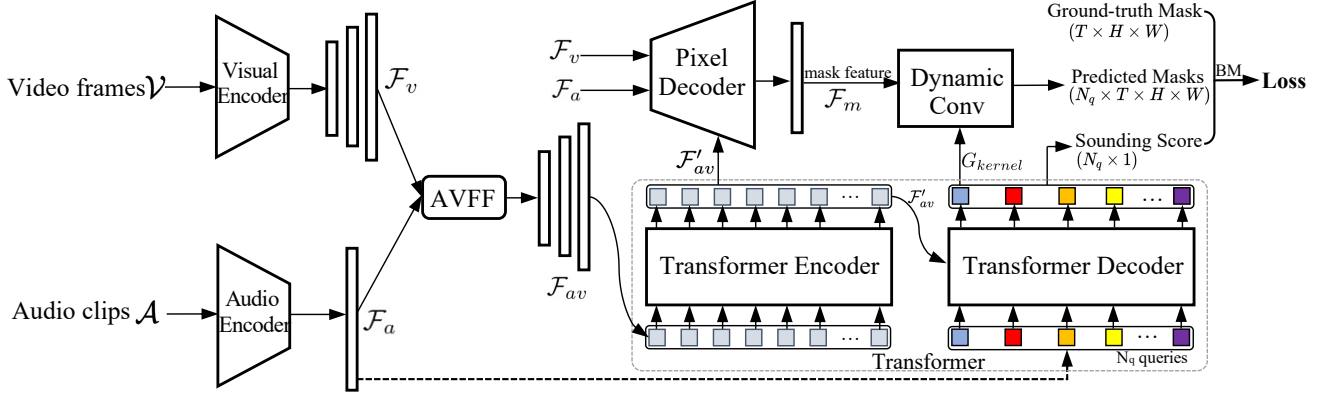


Figure 2: The architecture of **Audio-aware query-enhanced multi-modal TRansformer (AuTR)**. AuTR consists of six components: visual encoder and audio encoder to extract features, audio-visual feature fusion (AVFF), transformer including multi-modal encoder and audio-aware query-enhanced decoder, pixel decoder that outputs mask features, and dynamic convolutional block which predicts segmentations for all N_q queries. “BM” denotes *bipartite matching* in training stage.

3.3.2 Audio-Visual Feature Fusion

After obtaining the visual and audio features, we perform audio visual feature fusion that encourages the modality information interaction at early stage. In detail, we adopt MLP layers to adjust the dimension of audio features to C_{av} , and use 1×1 convolution to map the visual features of different scales to the dimension of C_{av} . In AVFF module (as shown in Figure 2), we leverage multi-head attention [55] between audio and visual features at each scale, with the queries coming from visual features while the audio features serving as keys and values. This multi-modal fusion between audio features and visual feature maps are conducted at each visual scale separately, ending up with multi-modal feature maps $\mathcal{F}_{av} = \{[f_1^t, f_2^t, f_3^t]\}_{t=1}^T$, where $f_\ell^t \in \mathbb{R}^{C_{av} \times H_\ell \times W_\ell}$, $\ell \in \{1, 2, 3\}$.

3.3.3 Audio-aware Multi-modal Transformer

Multi-modal Transformer Encoder. After multi-modal audio-visual fusion, the feature maps of different scales are flattened into sequence of tokens (with fixed spatial-temporal positional encoding added), and processed with transformer encoder, ending up with deeply fused cross-modal features, i.e., $\mathcal{F}'_{av} = \{[\hat{f}_1^t, \hat{f}_2^t, \hat{f}_3^t]\}_{t=1}^T$, where $\hat{f}_\ell^t \in \mathbb{R}^{C_{av} \times H_\ell \times W_\ell}$, $\ell \in \{1, 2, 3\}$.

Audio-aware Transformer Decoder. The transformer decoder aims to pinpoint the sounding object corresponding to the given audio with the cross-modal features, while ignoring the non-sounding objects and background. To achieve this, we present an audio-aware transformer decoder. Concretely, we first employ the patchified output embeddings (\mathcal{F}'_{av}) from transformer encoder by projecting them into *key* and *value* for the transformer decoder. As for

the queries, we endow the transformer decoder with audio-awareness by initialising a fixed number of N_q *audio-aware query vectors* that are computed from the extracted audio embeddings (\mathcal{F}_a) supplemented with learnable position embeddings. In this process, the transformer decoder transforms the N audio-aware learnable queries along with the multi-modal features to output embeddings for all query instances and iteratively attends the features to discover the sounding objects.

3.3.4 Mask Prediction

To obtain the target mask predictions, we leverage the dynamic convolution [53, 58] that encodes more instance-specific characteristics to perform segmentation instead of directly predicting the masks. Concretely, we first deploy a pixel decoder to aggregate the audio-visual multi-modal features into mask features, then use the dynamic convolutional block to predict the segmentation masks based on the mask features, detailed as follows.

Pixel Decoder. We construct a light-weight pixel decoder to obtain the mask features based on FPN [34] structure. The pixel decoder first accepts the multi-scale visual features \mathcal{F}_v from visual backbone, audio features \mathcal{F}_a from audio backbone, and the multi-modal audio-visual embeddings \mathcal{F}'_{av} from the transformer encoder, and aggregates these features with cross-attention and pooling operations. As a result, the enriched multi-modal features (\mathcal{F}_m) are used for segmentation, where $\mathcal{F}_m = \{f_m^t\}_{t=1}^T$, $f_m^t \in \mathbb{R}^{C_m \times H_m \times W_m}$.

Dynamic Convolution. The dynamic convolutional block depends on the output query embeddings to generate the convolution kernel weights for decoding the mask features into target masks. We denote the output sequence for all query instances from the transformer decoder as $\mathcal{F}_Q =$

$\{f_q^i\}_{i=1}^{N_q}$, where $f_q^i \in \mathbb{R}^D$. We employ two-layer MLPs to predict a series of weight parameters of convolutional kernels $G_{kernel} = \{k_i\}_{i=1}^{N_q}$. And the generated kernels are controlled by \mathcal{F}_Q :

$$\{k_i\}_{i=1}^{N_q} = g(\mathcal{F}_Q), \quad (1)$$

where $g(\cdot)$ denotes the kernel prediction function which is implemented with two-layer MLP.

Finally, we generate the prediction of target segmentation masks sequence $\hat{\mathcal{S}}$ for the sounding objects in the frame sequence by convolving the fused multi-modal mask features \mathcal{F}_m with the generated convolutional kernels G_{kernel} :

$$\hat{\mathcal{S}} = \mathcal{F}_m \star G_{kernel}, \quad (2)$$

where $\hat{\mathcal{S}} \in \mathbb{R}^{N_q \times T \times H_{lr} \times W_{lr}}$ are the predicted low-resolution segmentations for all queries.

3.3.5 Training

After acquiring segmentation masks for all the queries, we select the one that best refers to the sounding objects with bipartite matching strategy. Specifically, denoting the ground-truth segmentation mask as y and the predicted segmentation mask from our model as $\hat{\mathcal{Y}} = \{\hat{y}_i\}_{i=1}^{N_q}$. We find the best matched segmentations with the lowest cost to the ground-truth:

$$i^* = \underset{i \in \{1, \dots, N_q\}}{\operatorname{argmin}} \mathcal{C}(\hat{y}_i, y), \quad (3)$$

where \mathcal{C} is the pair-wise cost using certain metric, and i^* is the optimal query index. In addition to the segmentation head, we also append a binary classification head to map each query embedding to a single *sounding score* that represents the possibility of the existence of sounding objects corresponding to the audio queries.

The cost metrics \mathcal{C} in Eq. 3 consist of two parts: one for segmentation (\mathcal{C}_{seg}), that includes binary focal loss \mathcal{C}_{focal} and DICE loss [43] \mathcal{C}_{dice} , and the other is binary classification for sounding objects presence (\mathcal{C}_{sound}). The total loss function between query i and ground-truth can be written:

$$\mathcal{C}(\hat{s}_i, s) = \lambda_{dice}\mathcal{C}_{dice} + \lambda_{focal}\mathcal{C}_{focal} + \lambda_{sound}\mathcal{C}_{sound}, \quad (4)$$

where λ_{dice} , λ_{focal} and λ_{sound} are the weights to balance the costs. The whole framework is trained by minimizing the total cost between \hat{y}_{i^*} and ground-truth y .

3.3.6 Inference

At inference stage, given a video frame sequence and its corresponding audios, our model predicts the segmentation mask sequence for all query instances $\hat{\mathcal{Y}} = \{\hat{y}_i\}_{i=1}^{N_q}$, and corresponding sounding scores $z \in \{z_i\}_{i=1}^{N_q}$. We pick the

segmentation results with highest sounding score z , and use bilinear sampling to match the resolution sizes of ground-truth segmentation masks.

4. Experimental Settings

4.1. Datasets

AVSBench [68] is a newly released dataset for audio-visual segmentation that comes with human-annotated mask annotations. This dataset is divided into two subsets: the semi-supervised Single Sound Source Segmentation (S4) and the fully supervised Multiple Sound Source Segmentation (MS3).

AVSBench-S4 Dataset. This subset contains videos with a maximum of one sounding object. During training, only the first frame of the video sequence is annotated with a ground-truth segmentation binary mask. At inference time, the goal is to segment the sounding objects across all frames in the video. The subset includes 3,452/740/740 videos in the training, validation, and test sets, respectively, with a total of 10,852 annotated frames.

AVSBench-MS3 Dataset. The MS3 subset consists of videos that contain multiple sounding objects. All video frames are annotated with masks during both the training and evaluation stages. The subset contains 296/64/64 videos for training, validation and testing separately, with a total of 2,120 annotated frames.

AVS-Synthetic Dataset. As detailed in Section 3.2.1, AVS-Synthetic is a dataset collected using our proposed pipeline. The dataset includes 44 categories and contains over 60K (*image, audio, mask*) sample triplets. To facilitate training and evaluation, the dataset is divided into two splits: the training split, which includes 55,000 samples, and the test split, which includes 5,000 samples.

4.2. Metrics

In our approach, we utilize the standard segmentation measures outlined in [68]. Specifically, we use $\mathcal{M}_{\mathcal{J}}$ to calculate the mean Intersection-over-Union of ground-truth binary masks and predicted masks after thresholding, which provides a measure of region similarity. Additionally, we use $\mathcal{M}_{\mathcal{F}}$, also known as the F-score, which is the harmonic mean of precision and recall and measures contour accuracy. In both cases, higher values indicate better segmentation performance.

4.3. Implementation Details

We implemented our model using PyTorch and pre-trained the visual backbones, including ResNet50 and PVT-v2, on ImageNet [48]. The audio backbone, based on the VGGish model, was pretrained on AudioSet [18]. We froze the parameters of both the visual and audio backbones. For

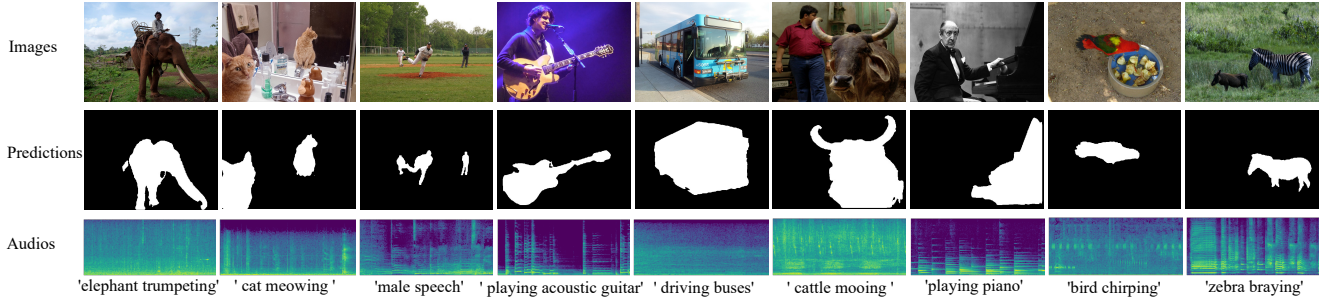


Figure 3: Qualitative results on the test split of AVS-Synthetic. In the third row, we show the input audio labels of VGGSound instead of audio spectrograms, we refer the readers to supplementary materials for the raw input audios.

Trained with	ambulance	cat	dog	bus	horse	lion	bird	guitar	piano	computer_keyboard	mean
Real	70.93	84.58	84.73	85.24	75.16	89.23	83.93	84.02	85.15	87.41	83.04
Synthetic	59.93	81.60	76.95	82.77	69.29	81.68	77.58	75.61	40.76	75.65	72.18

Table 2: Categorized results of direct evaluations of the models trained with synthetic data on real test data split of AVSBench (S4) [68]; The “Real” row means the model is trained with the real data of AVSBench training split; and the “Synthetic” row means the model is trained with AVS-Synthetic. Metric: $\mathcal{M}_{\mathcal{J}}$ (mIoU)

the AVS-Synthetic dataset experiments in Section 5.1, we selected PVT-v2 as the visual backbone. For the experiments on the proposed AuTR architecture in Section 5.2, we chose both ResNet50 and PVT-v2 to perform a comprehensive comparison against the baseline method AVS [68]. We used the Deformable Transformer [69] as the multi-modal transformer architecture in the framework for its efficiency. To optimize the models, we employed the AdamW [39] optimizer with an initial learning rate of 10^{-4} and weight decay of 5×10^{-4} . For training with the AVSBench dataset, we trained the models for 50 epochs using a single GeForce RTX 3090, and the training batch size was set to 8. The video frames were of 224×224 resolution. For training with the AVS-Synthetic dataset, we trained the models for 10 epochs using a single GeForce RTX 3090, and the training batch size was set to 1 since the images in the dataset have larger resolutions.

5. Experimental Results

In this section, we first presents our experimental results and analysis on our proposed AVS-Synthetic dataset. We then proceed to conduct extensive experiments to showcase the performance of our proposed AuTR framework on the public AVSBench dataset.

5.1. Effectiveness of AVS-Synthetic Dataset

We trained our proposed AuTR model on the training split of the AVS-Synthetic dataset and present results from three experimental settings: standard evaluation on the test split of AVS-Synthetic, zero-shot evaluation on the test split of AVSBench, and few-shot evaluation on the test split of

Real Training Data	w/o P.T.		w/ P.T.	
	$\mathcal{M}_{\mathcal{J}}$	$\mathcal{M}_{\mathcal{F}}$	$\mathcal{M}_{\mathcal{J}}$	$\mathcal{M}_{\mathcal{F}}$
0%	17.5	.254	61.7	.763
10%	70.8	.831	73.9	.845
20%	74.6	.852	75.6	.856
30%	75.2	.859	76.5	.866
100%	80.4	.890	80.3	.892

Table 3: Finetuning the model with different percentages of real training data from AVSBench dataset. “w/ P.T.” refers to the model pretrained on AVS-Synthetic. 0%, 10%, 20% and 30% are the ratios of real data from AVSBench S4 training set; while “w/o P.T.” means the normal training without using pretrained weights as initialization. The results show that the performance of the model trained on AVS-Synthetic can be further improved by finetuning with only a small amount of real data.

AVSBench after real data finetuning.

Results on Synthetic Dataset. In order to establish baselines for future research on the proposed AVS-Synthetic dataset, we trained the AuTR model using the training split of AVS-Synthetic with a PVT-v2 backbone. We then evaluated the model on the test split, achieving results of 47.18 on $\mathcal{M}_{\mathcal{J}}$ and 0.591 on $\mathcal{M}_{\mathcal{F}}$. Figure 3 provides qualitative results.

Zero-shot Results on Real Dataset. In this section, we present the evaluation of our model on real AVBench-S4 test split. Specifically, we trained the model on synthetic data and tested it on real videos. Table 2 showcases the re-

sults for the overlapping categories between AVS-Synthetic and AVSBench. While the model trained with synthetic data generally lags behind the one trained with real data, it achieves remarkably close results on numerous categories, such as “cat”, “bus” and “lion”. This demonstrates the effectiveness of our proposed data synthesis procedure, which enables zero-shot transfer to real data.

However, it is important to note that the model trained with synthetic data performs significantly worse than using real videos for some categories, such as “piano”. This may be attributed to the domain gap between different image/video datasets. Specifically, the video frames of the AVSBench dataset are from VGGSound and tend to be object-centric, while the image sets of AVS-Synthetic comprise LVIS and Open Images. Therefore, in future work, domain adaptation techniques should be investigated to alleviate this issue.

Data-efficient Adaptation with Real Data. To narrow the gap between synthetic and real data, we adopt a small amount of real training data from the AVSBench-S4 subset to fine-tune the model trained with AVS-Synthetic, creating a data-efficient few-shot learning scenario. The results, shown in Table 3, demonstrate that the model trained on AVS-Synthetic achieves 61.7 mIoU ($\mathcal{M}_{\mathcal{J}}$) without using any real data. However, by using only 10% of real data for fine-tuning, the performance can be significantly improved to 73.9 mIoU ($\mathcal{M}_{\mathcal{J}}$). We observe consistent improvement when more real data (20% and 30%) is provided for training. These results demonstrate that the model trained with synthetic data from our proposed pipeline can be further improved with real data, and the adaptation is highly data-efficient.

5.2. Effectiveness of AuTR Architecture

In this study, we conducted experiments on two subsets of AVSBench and compared the results with existing state-of-the-art methods in Section 5.2.1. To evaluate the generalization of our methods, we also conducted open set experiments in Section 5.2.2. In Section 5.2.3, we presented qualitative comparison results. To ensure a fair comparison, both AuTR and AVS were trained and evaluated on the real AVSBench dataset [68] with two subsets. Throughout all experiments, we did not utilize synthetic data pretraining in either method.

5.2.1 Comparison with State-of-the-art

In this study, we compare AuTR with the state-of-the-art AVS method [68], which is based on an encoder-fusion-decoder framework. Additionally, we consider other related audio-visual methods, including sound source localization (SSL) methods LVS [7] and MSSL [46], video object segmentation (VOS) methods 3DC [40] and SST [14],

Subsets		S4		MS3	
Methods		$\mathcal{M}_{\mathcal{J}}$	$\mathcal{M}_{\mathcal{F}}$	$\mathcal{M}_{\mathcal{J}}$	$\mathcal{M}_{\mathcal{F}}$
SSL	LVS [7]	37.9	.510	29.5	.330
	MSSL [46]	44.9	.663	26.1	.363
VOS	3DC [40]	57.1	.759	36.9	.503
	SST [14]	66.3	.801	42.6	.572
SOD	iGAN [41]	61.6	.778	42.9	.544
	LGVT [63]	74.9	.873	40.7	.593
AVS [68]	ResNet50	72.8	.848	47.9	.578
	PVT-v2	78.7	.879	54.0	.645
	PVT-v2 + F.T.	-	-	51.45	.671
AuTR	ResNet50	75.0	.852	49.4	.612
	PVT-v2	80.4	.891	56.2	.672
	PVT-v2 + F.T.	-	-	60.9	.725

Table 4: Comparison with the state-of-the-art method and other related audio-visual related methods on test sets of two subsets of AVSBench dataset. (“F.T.” denotes finetuning based on the pretrained weights on S4)

and salient object detection (SOD) methods iGAN [41] and LGVT [63].

According to the results presented in Table 4, our proposed approach outperforms existing methods in both subsets across all metrics. Despite achieving high values on the $\mathcal{M}_{\mathcal{J}}$ metric with ResNet50 and PVT-v2, the current AVS method [68] still falls short compared to our proposed method on the S4 subset. With ResNet50, our proposed method achieved a 2.2-point improvement over AVS, while with PVT-v2, it achieved a 1.7-point improvement. These results demonstrate the superiority of the audio-aware transformer over the fusion-based model [68].

Moreover, our analysis indicates that the performance of all methods is notably inferior on the MS3 subset as compared to the S4 subset. To address this issue, we fine-tuned the models that had already been trained on the S4 subset on the MS3 subset. The results of the AVS and AuTR models are presented in the “PVT-v2 + F.T.” rows of Table 4. The results demonstrate that pre-training on the S4 subset significantly improved the performance of AuTR on the MS3 subset, resulting in a 4.74 *improvement*. However, the AVS [68] model’s performance on the MS3 subset dropped by 3.55 *points*. These findings indicate that our proposed AuTR architecture enables leveraging knowledge from single sound scenarios to improve performance on multiple sound scenes. Overall, our experiments demonstrate the effectiveness of the proposed AuTR architecture, which outperforms existing state-of-the-art approaches across all experimental settings.

5.2.2 Open Set Audio Visual Segmentation

Up until this point, audio-visual segmentation models on both S4 and MS3 subsets have been trained and tested un-

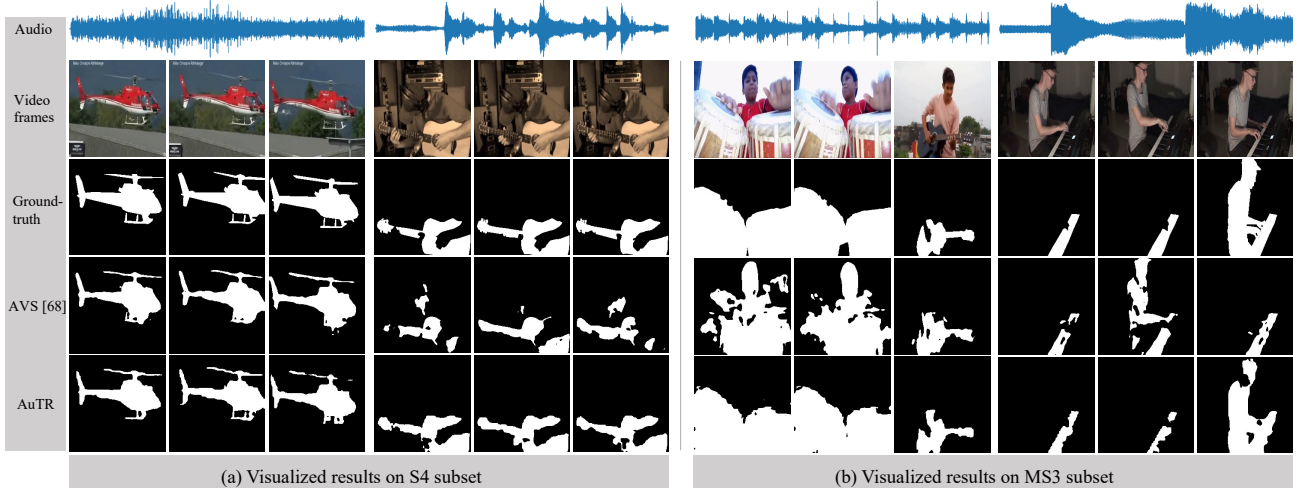


Figure 4: Qualitative results of AVS [68] and our proposed AuTR on the test set of S4 and MS3 subsets of AVSBench.

der a close-set scenario, where all categories for training and testing remain the same. In this section, we explore open-set segmentation, which involves training on partial categories and testing on disjoint categories. Specifically, we randomly sampled 11 categories of videos from the S4 subset for training and validation (seen categories), then tested on the other 12 categories (unseen categories). We compared the open-set performance between the AVS [68] method and our proposed AuTR method.

Table 5 shows that on seen categories, both methods achieved decent results, with our model outperforming AVS in both metrics. However, when evaluating on unseen categories, both methods experienced a performance drop. For example, the results of $\mathcal{M}_{\mathcal{J}}$ dropped from 75.62 to 55.86 for AVS [68] and from 77.56 to 66.22 for our model. Despite this, our method still performed better than AVS [68] with PVT-v2 backbone on $\mathcal{M}_{\mathcal{J}}$ by 10.36 points, demonstrating the strong generalization of our proposed AuTR architecture.

Method	Backbones	Seen categories		Unseen categories	
		$\mathcal{M}_{\mathcal{J}}$	$\mathcal{M}_{\mathcal{F}}$	$\mathcal{M}_{\mathcal{J}}$	$\mathcal{M}_{\mathcal{F}}$
AVS	ResNet50	68.93	.815	47.46	.683
	PVT-v2	75.62	.862	55.86	.719
AuTR	ResNet50	70.46	.817	51.15	.675
	PVT-v2	77.56	.865	66.22	.777

Table 5: Open set segmentation performance comparison between AVS [68] and our proposed AuTR.

5.2.3 Qualitative Examples

In Figure 4, we present qualitative segmentation results of AVS [68] and our method on the two subsets. Notably, our AuTR model demonstrates superior performance in localiz-

ing and segmenting sounding objects on the S4 subset. Furthermore, in challenging multi-sound scenarios, our method accurately segments the target sounding objects while disregarding distracting objects. In contrast, AVS [68] tends to overlook audio cues and segment even silent yet salient objects in some frames.

6. Conclusion

To summarise, this paper presents a novel pipeline for creating a synthetic dataset for the task of Audio-Visual Segmentation (AVS). The pipeline is based on off-the-shelf image segmentation datasets and audio corpus, and it offers an *annotation-free* and *scalable* alternative to traditional, labor-intensive annotation procedures. We also introduce a new architecture called AuTR, which leverages a multi-modal transformer to facilitate the fusion of multi-modal features. The architecture uses audio-guided queries to iteratively attend to visual features and ground sounding objects. Our extensive experiments demonstrate the effectiveness of both the proposed dataset synthesis pipeline and the AuTR architecture.

Moving forward, we plan to explore the use of open-vocabulary segmentors, such as SAM [29], to generate sounding objects from a more diverse range of categories. This would address the issue of limited sounding categories in current image segmentation datasets.

References

- [1] Anurag Arnab, Mostafa Dehghani, Georg Heigold, Chen Sun, Mario Lučić, and Cordelia Schmid. Vivit: A video vision transformer. In *Proceedings of the IEEE/CVF International Conference on Computer Vision*, pages 6836–6846, 2021.

- [2] Gedas Bertasius, Heng Wang, and Lorenzo Torresani. Is space-time attention all you need for video understanding? In *ICML*, volume 2, page 4, 2021.
- [3] Adam Botach, Evgenii Zheltonozhskii, and Chaim Baskin. End-to-end referring video object segmentation with multi-modal transformers. In *Proceedings of the IEEE/CVF Conference on Computer Vision and Pattern Recognition*, pages 4985–4995, 2022.
- [4] Nicolas Carion, Francisco Massa, Gabriel Synnaeve, Nicolas Usunier, Alexander Kirillov, and Sergey Zagoruyko. End-to-end object detection with transformers. In *European conference on computer vision*, pages 213–229. Springer, 2020.
- [5] Mathilde Caron, Hugo Touvron, Ishan Misra, Hervé Jégou, Julien Mairal, Piotr Bojanowski, and Armand Joulin. Emerging properties in self-supervised vision transformers. In *Proceedings of the IEEE/CVF International Conference on Computer Vision*, pages 9650–9660, 2021.
- [6] Hanting Chen, Yunhe Wang, Tianyu Guo, Chang Xu, Yiping Deng, Zhenhua Liu, Siwei Ma, Chunjing Xu, Chao Xu, and Wen Gao. Pre-trained image processing transformer. In *Proceedings of the IEEE/CVF Conference on Computer Vision and Pattern Recognition*, pages 12299–12310, 2021.
- [7] Honglie Chen, Weidi Xie, Triantafyllos Afouras, Arsha Nagrani, Andrea Vedaldi, and Andrew Zisserman. Localizing visual sounds the hard way. In *Proceedings of the IEEE/CVF Conference on Computer Vision and Pattern Recognition*, pages 16867–16876, 2021.
- [8] Honglie Chen, Weidi Xie, Andrea Vedaldi, and Andrew Zisserman. Vggsound: A large-scale audio-visual dataset. In *ICASSP 2020-2020 IEEE International Conference on Acoustics, Speech and Signal Processing (ICASSP)*, pages 721–725. IEEE, 2020.
- [9] Weidong Chen, Dexiang Hong, Yuankai Qi, Zhenjun Han, Shuhui Wang, Laiyun Qing, Qingming Huang, and Guorong Li. Multi-attention network for compressed video referring object segmentation. In *Proceedings of the 30th ACM International Conference on Multimedia*, pages 4416–4425, 2022.
- [10] Xin Chen, Bin Yan, Jiawen Zhu, Dong Wang, Xiaoyun Yang, and Huchuan Lu. Transformer tracking. In *Proceedings of the IEEE/CVF Conference on Computer Vision and Pattern Recognition*, pages 8126–8135, 2021.
- [11] Bowen Cheng, Ishan Misra, Alexander G. Schwing, Alexander Kirillov, and Rohit Girdhar. Masked-attention mask transformer for universal image segmentation. In *Proceedings of the IEEE/CVF Conference on Computer Vision and Pattern Recognition (CVPR)*, pages 1290–1299, June 2022.
- [12] Bowen Cheng, Alex Schwing, and Alexander Kirillov. Pixel classification is not all you need for semantic segmentation. *Advances in Neural Information Processing Systems*, 34:17864–17875, 2021.
- [13] Zhigang Dai, Bolun Cai, Yugeng Lin, and Junying Chen. Up-detr: Unsupervised pre-training for object detection with transformers. In *Proceedings of the IEEE/CVF conference on computer vision and pattern recognition*, pages 1601–1610, 2021.
- [14] Brendan Duke, Abdalla Ahmed, Christian Wolf, Parham Aarabi, and Graham W Taylor. Sstvos: Sparse spatiotemporal transformers for video object segmentation. In *Proceedings of the IEEE/CVF Conference on Computer Vision and Pattern Recognition*, pages 5912–5921, 2021.
- [15] Ariel Ephrat, Inbar Mosseri, Oran Lang, Tali Dekel, Kevin Wilson, Avinandan Hassidim, William T. Freeman, and Michael Rubinstein. Looking to listen at the cocktail party: a speaker-independent audio-visual model for speech separation. *ACM Trans. Graph.*, 37(4):112, 2018.
- [16] Peng Gao, Minghang Zheng, Xiaogang Wang, Jifeng Dai, and Hongsheng Li. Fast convergence of detr with spatially modulated co-attention. In *Proceedings of the IEEE/CVF International Conference on Computer Vision*, pages 3621–3630, 2021.
- [17] Ruohan Gao and Kristen Grauman. Visualvoice: Audio-visual speech separation with cross-modal consistency. In *2021 IEEE/CVF Conference on Computer Vision and Pattern Recognition (CVPR)*, pages 15490–15500. IEEE, 2021.
- [18] Jort F Gemmeke, Daniel PW Ellis, Dylan Freedman, Aren Jansen, Wade Lawrence, R Channing Moore, Manoj Plakal, and Marvin Ritter. Audio set: An ontology and human-labeled dataset for audio events. In *2017 IEEE international conference on acoustics, speech and signal processing (ICASSP)*, pages 776–780. IEEE, 2017.
- [19] Agrim Gupta, Piotr Dollar, and Ross Girshick. Lvis: A dataset for large vocabulary instance segmentation. In *Proceedings of the IEEE/CVF conference on computer vision and pattern recognition*, pages 5356–5364, 2019.
- [20] Akshita Gupta, Sanath Narayan, KJ Joseph, Salman Khan, Fahad Shahbaz Khan, and Mubarak Shah. Ow-detr: Open-world detection transformer. In *Proceedings of the IEEE/CVF Conference on Computer Vision and Pattern Recognition*, pages 9235–9244, 2022.
- [21] Kaiming He, Xinlei Chen, Saining Xie, Yanghao Li, Piotr Dollár, and Ross Girshick. Masked autoencoders are scalable vision learners. In *Proceedings of the IEEE/CVF Conference on Computer Vision and Pattern Recognition*, pages 16000–16009, 2022.
- [22] Kaiming He, Xiangyu Zhang, Shaoqing Ren, and Jian Sun. Deep residual learning for image recognition. In *Proceedings of the IEEE conference on computer vision and pattern recognition*, pages 770–778, 2016.
- [23] Shawn Hershey, Sourish Chaudhuri, Daniel PW Ellis, Jort F Gemmeke, Aren Jansen, R Channing Moore, Manoj Plakal, Devin Platt, Rif A Saurous, Bryan Seybold, et al. Cnn architectures for large-scale audio classification. In *2017 IEEE international conference on acoustics, speech and signal processing (icassp)*, pages 131–135. IEEE, 2017.
- [24] Di Hu, Feiping Nie, and Xuelong Li. Deep multimodal clustering for unsupervised audiovisual learning. In *Proceedings of the IEEE/CVF Conference on Computer Vision and Pattern Recognition*, pages 9248–9257, 2019.
- [25] Di Hu, Rui Qian, Minyue Jiang, Xiao Tan, Shilei Wen, Errui Ding, Weiyao Lin, and Dejing Dou. Discriminative sounding objects localization via self-supervised audiovisual matching. *Advances in Neural Information Processing Systems*, 33:10077–10087, 2020.
- [26] Di Hu, Yake Wei, Rui Qian, Weiyao Lin, Ruihua Song, and Ji-Rong Wen. Class-aware sounding objects localization via

- audiovisual correspondence. *IEEE Transactions on Pattern Analysis and Machine Intelligence*, 2021.
- [27] Aishwarya Kamath, Mannat Singh, Yann LeCun, Gabriel Synnaeve, Ishan Misra, and Nicolas Carion. Mdetr-modulated detection for end-to-end multi-modal understanding. In *Proceedings of the IEEE/CVF International Conference on Computer Vision*, pages 1780–1790, 2021.
 - [28] Evangelos Kazakos, Arsha Nagrani, Andrew Zisserman, and Dima Damen. Epic-fusion: Audio-visual temporal binding for egocentric action recognition. In *Proceedings of the IEEE/CVF International Conference on Computer Vision*, pages 5492–5501, 2019.
 - [29] Alexander Kirillov, Eric Mintun, Nikhila Ravi, Hanzi Mao, Chloe Rolland, Laura Gustafson, Tete Xiao, Spencer Whitehead, Alexander C Berg, Wan-Yen Lo, et al. Segment anything. *arXiv preprint arXiv:2304.02643*, 2023.
 - [30] Alina Kuznetsova, Hassan Rom, Neil Alldrin, Jasper Uijlings, Ivan Krasin, Jordi Pont-Tuset, Shahab Kamali, Stefan Popov, Matteo Mallocci, Alexander Kolesnikov, et al. The open images dataset v4: Unified image classification, object detection, and visual relationship detection at scale. *International Journal of Computer Vision*, 128(7):1956–1981, 2020.
 - [31] Jun-Tae Lee, Mihir Jain, Hyoungwoo Park, and Sungrack Yun. Cross-attentional audio-visual fusion for weakly-supervised action localization. In *International Conference on Learning Representations*, 2020.
 - [32] Xiang Li, Jinglu Wang, Xiaohao Xu, Xiao Li, Yan Lu, and Bhiksha Raj. R²vos: Robust referring video object segmentation via relational multimodal cycle consistency. *CoRR*, abs/2207.01203, 2022.
 - [33] Zhiqi Li, Wenhao Wang, Enze Xie, Zhiding Yu, Anima Anandkumar, Jose M Alvarez, Ping Luo, and Tong Lu. Panoptic segformer: Delving deeper into panoptic segmentation with transformers. In *Proceedings of the IEEE/CVF Conference on Computer Vision and Pattern Recognition*, pages 1280–1289, 2022.
 - [34] Tsung-Yi Lin, Piotr Dollár, Ross Girshick, Kaiming He, Bharath Hariharan, and Serge Belongie. Feature pyramid networks for object detection. In *Proceedings of the IEEE conference on computer vision and pattern recognition*, pages 2117–2125, 2017.
 - [35] Yan-Bo Lin, Hung-Yu Tseng, Hsin-Ying Lee, Yen-Yu Lin, and Ming-Hsuan Yang. Unsupervised sound localization via iterative contrastive learning. *CoRR*, abs/2104.00315, 2021.
 - [36] Yan-Bo Lin, Yu-Jhe Li, and Yu-Chiang Frank Wang. Dual-modality seq2seq network for audio-visual event localization. In *ICASSP 2019-2019 IEEE International Conference on Acoustics, Speech and Signal Processing (ICASSP)*, pages 2002–2006. IEEE, 2019.
 - [37] Jinxiang Liu, Chen Ju, Weidi Xie, and Ya Zhang. Exploiting transformation invariance and equivariance for self-supervised sound localisation. In *Proceedings of the 30th ACM International Conference on Multimedia*, pages 3742–3753, 2022.
 - [38] Ze Liu, Yutong Lin, Yue Cao, Han Hu, Yixuan Wei, Zheng Zhang, Stephen Lin, and Baining Guo. Swin transformer: Hierarchical vision transformer using shifted windows. In *Proceedings of the IEEE/CVF International Conference on Computer Vision*, pages 10012–10022, 2021.
 - [39] Ilya Loshchilov and Frank Hutter. Decoupled weight decay regularization. *arXiv preprint arXiv:1711.05101*, 2017.
 - [40] Sabarinath Mahadevan, Ali Athar, Aljosa Osep, Laura Leal-Taixé, Bastian Leibe, and Sebastian Hennen. Making a case for 3d convolutions for object segmentation in videos. In *31st British Machine Vision Conference 2020, BMVC 2020, Virtual Event, UK, September 7-10, 2020*. BMVA Press, 2020.
 - [41] Yuxin Mao, Jing Zhang, Zhexiong Wan, Yuchao Dai, Aixuan Li, Yunqiu Lv, Xinyu Tian, Deng-Ping Fan, and Nick Barnes. Transformer transforms salient object detection and camouflaged object detection. *CoRR*, abs/2104.10127, 2021.
 - [42] Tim Meinhardt, Alexander Kirillov, Laura Leal-Taixé, and Christoph Feichtenhofer. Trackformer: Multi-object tracking with transformers. In *Proceedings of the IEEE/CVF Conference on Computer Vision and Pattern Recognition*, pages 8844–8854, 2022.
 - [43] Fausto Milletari, Nassir Navab, and Seyed-Ahmad Ahmadi. V-net: Fully convolutional neural networks for volumetric medical image segmentation. In *2016 fourth international conference on 3D vision (3DV)*, pages 565–571. IEEE, 2016.
 - [44] Andrew Owens and Alexei A Efros. Audio-visual scene analysis with self-supervised multisensory features. In *Proceedings of the European Conference on Computer Vision (ECCV)*, pages 631–648, 2018.
 - [45] Mandela Patrick, Dylan Campbell, Yuki Asano, Ishan Misra, Florian Metze, Christoph Feichtenhofer, Andrea Vedaldi, and João F Henriques. Keeping your eye on the ball: Trajectory attention in video transformers. *Advances in neural information processing systems*, 34:12493–12506, 2021.
 - [46] Rui Qian, Di Hu, Heinrich Dinkel, Mengyue Wu, Ning Xu, and Weiyao Lin. Multiple sound sources localization from coarse to fine. In *European Conference on Computer Vision*, pages 292–308. Springer, 2020.
 - [47] René Ranftl, Alexey Bochkovskiy, and Vladlen Koltun. Vision transformers for dense prediction. In *Proceedings of the IEEE/CVF International Conference on Computer Vision*, pages 12179–12188, 2021.
 - [48] Olga Russakovsky, Jia Deng, Hao Su, Jonathan Krause, Sanjeev Satheesh, Sean Ma, Zhiheng Huang, Andrej Karpathy, Aditya Khosla, Michael Bernstein, et al. Imagenet large scale visual recognition challenge. *International journal of computer vision*, 115:211–252, 2015.
 - [49] Arda Senocak, Tae-Hyun Oh, Junsik Kim, Ming-Hsuan Yang, and In So Kweon. Learning to localize sound source in visual scenes. In *Proceedings of the IEEE Conference on Computer Vision and Pattern Recognition*, pages 4358–4366, 2018.
 - [50] Zengjie Song, Yuxi Wang, Junsong Fan, Tieniu Tan, and Zhaoxiang Zhang. Self-supervised predictive learning: A negative-free method for sound source localization in visual scenes. In *Proceedings of the IEEE/CVF Conference on Computer Vision and Pattern Recognition*, pages 3222–3231, 2022.
 - [51] Peize Sun, Yi Jiang, Rufeng Zhang, Enze Xie, Jinkun Cao, Xinting Hu, Tao Kong, Zehuan Yuan, Changhu Wang, and

- Ping Luo. Transtrack: Multiple-object tracking with transformer. *CoRR*, abs/2012.15460, 2020.
- [52] Yapeng Tian, Dingzeyu Li, and Chenliang Xu. Unified multisensory perception: Weakly-supervised audio-visual video parsing. In *European Conference on Computer Vision*, pages 436–454. Springer, 2020.
- [53] Zhi Tian, Chunhua Shen, and Hao Chen. Conditional convolutions for instance segmentation. In *European conference on computer vision*, pages 282–298. Springer, 2020.
- [54] Efthymios Tzinis, Scott Wisdom, Tal Remez, and John R. Hershey. Audioscopev2: Audio-visual attention architectures for calibrated open-domain on-screen sound separation. In Shai Avidan, Gabriel J. Brostow, Moustapha Cissé, Giovanni Maria Farinella, and Tal Hassner, editors, *Computer Vision - ECCV 2022 - 17th European Conference, Tel Aviv, Israel, October 23-27, 2022, Proceedings, Part XXXVII*, volume 13697 of *Lecture Notes in Computer Science*, pages 368–385. Springer, 2022.
- [55] Ashish Vaswani, Noam Shazeer, Niki Parmar, Jakob Uszkoreit, Llion Jones, Aidan N Gomez, Łukasz Kaiser, and Illia Polosukhin. Attention is all you need. *Advances in neural information processing systems*, 30, 2017.
- [56] Wenhai Wang, Enze Xie, Xiang Li, Deng-Ping Fan, Kaitao Song, Ding Liang, Tong Lu, Ping Luo, and Ling Shao. Pyramid vision transformer: A versatile backbone for dense prediction without convolutions. In *Proceedings of the IEEE/CVF International Conference on Computer Vision*, pages 568–578, 2021.
- [57] Wenhai Wang, Enze Xie, Xiang Li, Deng-Ping Fan, Kaitao Song, Ding Liang, Tong Lu, Ping Luo, and Ling Shao. Pvt v2: Improved baselines with pyramid vision transformer. *Computational Visual Media*, 8(3):415–424, 2022.
- [58] Xinlong Wang, Rufeng Zhang, Tao Kong, Lei Li, and Chunhua Shen. Solov2: Dynamic and fast instance segmentation. *Advances in Neural information processing systems*, 33:17721–17732, 2020.
- [59] Yuqing Wang, Zhaoliang Xu, Xinlong Wang, Chunhua Shen, Baoshan Cheng, Hao Shen, and Huaxia Xia. End-to-end video instance segmentation with transformers. In *Proceedings of the IEEE/CVF Conference on Computer Vision and Pattern Recognition*, pages 8741–8750, 2021.
- [60] Junfeng Wu, Yi Jiang, Song Bai, Wenqing Zhang, and Xiang Bai. Seqformer: Sequential transformer for video instance segmentation. *Computer Vision ECCV*, 2022.
- [61] Jiannan Wu, Yi Jiang, Peize Sun, Zehuan Yuan, and Ping Luo. Language as queries for referring video object segmentation. In *Proceedings of the IEEE/CVF Conference on Computer Vision and Pattern Recognition*, pages 4974–4984, 2022.
- [62] Bin Yan, Houwen Peng, Jianlong Fu, Dong Wang, and Huchuan Lu. Learning spatio-temporal transformer for visual tracking. In *Proceedings of the IEEE/CVF International Conference on Computer Vision (ICCV)*, pages 10448–10457, October 2021.
- [63] Jing Zhang, Jianwen Xie, Nick Barnes, and Ping Li. Learning generative vision transformer with energy-based latent space for saliency prediction. *Advances in Neural Information Processing Systems*, 34:15448–15463, 2021.
- [64] Hang Zhao, Chuang Gan, Wei-Chiu Ma, and Antonio Torralba. The sound of motions. In *Proceedings of the IEEE/CVF International Conference on Computer Vision*, pages 1735–1744, 2019.
- [65] Hang Zhao, Chuang Gan, Andrew Rouditchenko, Carl Vondrick, Josh McDermott, and Antonio Torralba. The sound of pixels. In *Proceedings of the European conference on computer vision (ECCV)*, pages 570–586, 2018.
- [66] Sixiao Zheng, Jiachen Lu, Hengshuang Zhao, Xiatian Zhu, Zekun Luo, Yabiao Wang, Yanwei Fu, Jianfeng Feng, Tao Xiang, Philip HS Torr, et al. Rethinking semantic segmentation from a sequence-to-sequence perspective with transformers. In *Proceedings of the IEEE/CVF conference on computer vision and pattern recognition*, pages 6881–6890, 2021.
- [67] Bolei Zhou, Aditya Khosla, Agata Lapedriza, Aude Oliva, and Antonio Torralba. Learning deep features for discriminative localization. In *Proceedings of the IEEE conference on computer vision and pattern recognition*, pages 2921–2929, 2016.
- [68] Jinxing Zhou, Jianyuan Wang, Jiayi Zhang, Weixuan Sun, Jing Zhang, Stan Birchfield, Dan Guo, Lingpeng Kong, Meng Wang, and Yiran Zhong. Audio-visual segmentation. In *European Conference on Computer Vision*, 2022.
- [69] Xizhou Zhu, Weijie Su, Lewei Lu, Bin Li, Xiaogang Wang, and Jifeng Dai. Deformable DETR: deformable transformers for end-to-end object detection. In *9th International Conference on Learning Representations, ICLR 2021, Virtual Event, Austria, May 3-7, 2021*. OpenReview.net, 2021.